Artificial Neural Network Model for HEMTs Constructed from Large-Signal Time-Domain Measurements*

Dominique M. M.-P. Schreurs[1], Jeffrey A. Jargon[2],
Kate A. Remley[2], Donald C. DeGroot[2], and K.C. Gupta[3]

[1]K.U.Leuven, Div. ESAT-TELEMIC, Kasteelpark Arenberg 10, B-3001 Leuven, Belgium
Phone: +32-16-321821, Fax: +32-16-321986, E-mail: Dominique.Schreurs@esat.kuleuven.ac.be
[2]National Institute of Standards and Technology, 325 Broadway, Boulder, CO 80305, USA
[3]University of Colorado, Dept. of Electrical and Computer Eng., Boulder, CO 80309, USA

Abstract

A methodology to construct behavioural models for microwave devices from time-domain large-signal measurements has been modified by using artificial neural networks (ANNs) for the multivariate fitting functions instead of polynomials. The behavioural models for the class of devices (microwave transistors) considered can be defined by expressing the terminal currents as functions of the state variables, the embedded voltages. In this work, we show that ANNs are valuable candidates to represent these relationships. They outperform models based on multivariate polynomials, because they can better model the typical physical characteristics of the devices considered. Experimental results are quantitatively confirmed by using comparison metrics.

I. Introduction

Large-signal models for microwave devices are classically derived by an indirect method requiring the use of small-signal S-parameter measurements. Due to recent advances in the metrology of *vectorial large-signal* measurements [1]-[4], several novel modelling methodologies that circumvent this small-signal indirect method are being developed. Some examples of such modelling techniques include parametric equivalent-circuit model extraction [5]-[7], and behavioural model identifications in the frequency domain [7]-[8]. Recently, we proposed a procedure to construct a *time-domain* behavioural model [9], where we built upon techniques developed in nonlinear time-series analysis (NLTSA) [10].

In this modelling method, an electrical two-port can be described by the general equations of the form [9]

$$\begin{aligned} I_1(t) &= f_1\left(V_1(t), V_2(t), \dot{V}_1(t), \dot{V}_2(t), \ddot{V}_1(t), \ddot{V}_2(t), \cdots, \dot{I}_1(t), \dot{I}_2(t), \cdots\right) \\ I_2(t) &= f_2\left(V_1(t), V_2(t), \dot{V}_1(t), \dot{V}_2(t), \ddot{V}_1(t), \ddot{V}_2(t), \cdots, \dot{I}_1(t), \dot{I}_2(t), \cdots\right) \end{aligned} \tag{1}$$

with $I_1(t)$ and $I_2(t)$ the terminal currents, and $V_1(t)$ and $V_2(t)$ the terminal voltages. For the considered class of devices, microwave transistors, the terminal currents are mostly functions of the terminal voltages and their higher order derivatives only. The feedback components, being the higher order derivatives of the terminal currents, only become important in case of non-linear inductive effects, which are rarely encountered in microwave transistors.

The objective of the modelling technique is to find the functional relationships $f_1(.)$ and $f_2(.)$ by fitting the measured terminal currents to the measured independent variables or state variables. In this work, we evaluate the use of ANNs as fitting functions.

*Work partially supported by U.S. Government.

0-7803-7143-7/02/$10.00 ©2002 IEEE.

In Section II, we describe in detail the construction of the ANN-based model. The different steps are clarified by applying them to a high-electron-mobility transistor (HEMT). Next, the accuracy of the ANN model is compared to that of a model based on multivariate polynomials. Section III covers DC and large-signal results, whereas comparison metrics to quantify these differences are introduced and applied to our study in Section IV. Finally, conclusions are drawn in Section V.

II. ANN Model Construction

The model is built from time domain data, obtained by performing vectorial large-signal measurements using a nonlinear network measurement system (NNMS) [4]. At the start of the modelling process, operating bounds for the model are established by defining the minimum and maximum values of the state variables. These bounds define the operating region within the state space for which the model is to be developed and used. To enable practical identification of the device dynamics, the measured time domain data need to sample this operating region efficiently. However, since the actual state variables are unknown at the start, we begin by defining the minimum and maximum values of the terminal voltages, V_1 and V_2. To find the other state-variables, we use an embedding process (described below) on the time domain data collected. If it turns out after the embedding process that there is not yet sufficient variation in the other state variables ($\dot{V}_1, \dot{V}_2$, ...), we may need to iterate between this measurement and the embedding parts.

Recently, we presented a method that enables us to automatically calculate the excitation signals we need to apply, in order to efficiently cover the predefined operating (V_1, V_2) voltage space of a (quasi-) unilateral microwave two-port device [11]. We tested the method on a HEMT device, for which we intended to cover the rectangle defined by the (V_1, V_2) points (-0.8 V, 0 V) and (0 V, 1 V) and found that 27 vectorial large-signal measurements were sufficient to cover the predefined operating region. The same HEMT device is studied in the present work.

Since the behavioural modelling approach supposes that no physical background information is available, we have to determine the independent (or state) variables. This can be accomplished by the so-called "embedding" technique, based on the "false nearest neighbour" principle [12]. The basic principle of the embedding technique is to unfold the characteristics of the dependent variables I_1 and I_2 in an increasing dimensional space by increasing the number of independent variables $\left(V_1(t), V_2(t), \dot{V}_1(t), \dot{V}_2(t), \ddot{V}_1(t), \ddot{V}_2(t), \cdots\right)$ until a single-valued function for each current is obtained. By applying this technique to the measured data of the HEMT studied, we found we must include state variables up to the 2nd derivative of $V_1(t)$ and $V_2(t)$, for both I_1 and I_2. Also, the inclusion of the derivatives of the terminal currents was not necessary.

Finally, the functional relationships $f_1(.)$ and $f_2(.)$ are determined by fitting the measured time domain terminal currents to the measured independent variables, determined in the preceding step. As a fitting function, we used an artificial neural network (ANN) with 6 inputs (the voltages up to the second derivative) and two outputs (the currents). We found that an ANN with a single hidden layer of 30 neurons provides the best trade-off between model accuracy and model complexity. The activation function of the hidden neurons is the sigmoid function. The ANN has first been trained using the back-propagation algorithm, and has consequently been fine-tuned using the quasi-Newton method, as implemented in the software developed by Prof. Zhang *et al.*, described in detail in Refs. [13]-[15].

III. DC and Large-Signal Results

We implemented our time-domain behavioural model of the HEMT device in a commercial microwave circuit simulator by means of a symbolically defined device (SDD). The SDD can determine the time-derivatives of the terminal voltages at each time-step in the simulation, enabling the fitting functions for the currents to be evaluated.

We validated the model using large-signal measurements. Figure 1 shows the agreement between measured and simulated time-domain waveforms of the terminal currents and voltages. The experimental conditions are listed in the caption. The simulations were carried out at exactly the same excitation conditions as the measurements.

As way of comparison, we also constructed a model based on the same set of 27 vectorial large-signal measurements, but with multivariate polynomials used to describe $f_1(.)$ and $f_2(.)$. The polynomial coefficients were determined using a least squares fitting procedure.

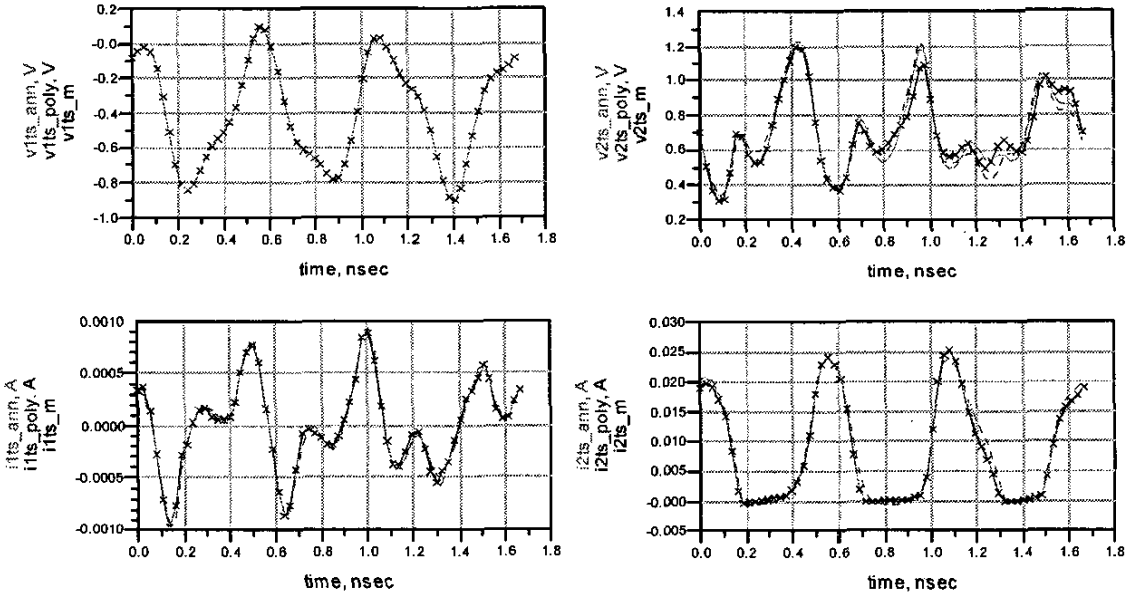

Fig. 1. Comparison of the measured (x), ANN- (solid line) and polynomial-based (dashed line) simulations of the time domain waveforms of the terminal currents and voltages (V_{gsDC} = -0.4 V, V_{dsDC} = 0.7 V, f_0=1.8 GHz, a_1= -3.9 dBm (with a secondary excitation at port 1 of -15.4 dBm at 4.2 GHz), a_2= -0.7 dBm, $\phi(a_2)$-$\phi(a_1)$=22°).

The simulation results using this polynomial-based model are also shown in Figure 1. We notice that both representations (ANNs and polynomials) agree well with the measurements. However, the ANN-based model outperforms the polynomial-based model, especially at the instantaneous conditions were the drain-source current is cut-off. This is represented more clearly in Figure 2, which shows the absolute difference between the simulated and measured I_2 time-domain waveforms, for the two respective models. The order of the considered multivariate polynomial is 3. A higher order polynomial in general improves the accuracy at higher current values, but also increases the "ringing" effect at cut-off conditions.

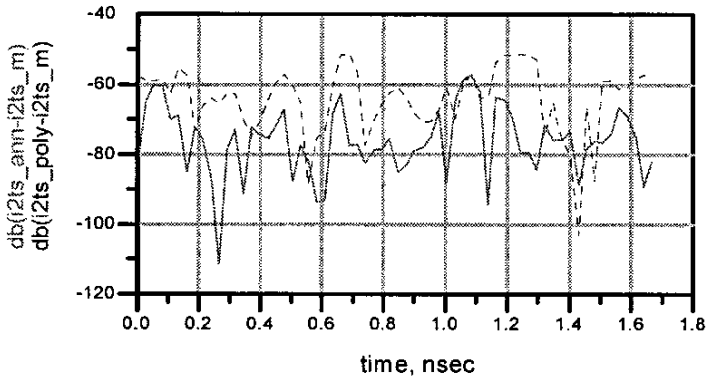

Fig. 2. Differences between measured and corresponding ANN- (solid line) and polynomial-based (dashed line) simulated I_2 time domain waveforms.

Better agreement between measurements and the ANN-based model is attributed to the fact that the weighted combination of sigmoid activation functions, upon which our ANN model is based, better models the typical physical characteristics of a microwave transistor. This agreement is also reflected in the simulated DC I-V characteristics, shown in Figs. 3 and 4. The DC behaviour of the model arises from effectively setting all the derivative terms to zero in the functional equations for $f_1(.)$ and $f_2(.)$. The resulting I-V curves are then determined by the static non-linearities in the functions of V_1 and V_2. We concentrate on two limiting conditions: cut-off (where V_{gsDC} < threshold voltage), and the case where V_{dsDC} equals 0 V. We see that the polynomial model predicts a negative current below the threshold voltage (Figure 3), as well as a nonzero current at V_{dsDC} equal to 0 V (Figure 4), which are not physical. These limiting conditions can be better controlled using an ANN due to the natural bounds and shape of the sigmoid activation function. Note that DC, as well as small-signal (= S-parameters), measurements were not explicitly used to construct our behavioural model.

The results on using ANNs instead of multivariate polynomials for the purpose of behavioural modelling of microwave transistors are in agreement with those obtained, independently, by other researchers [16].

In the next section, we will quantify these differences in accuracy of the ANN- and polynomial-based models using comparison metrics.

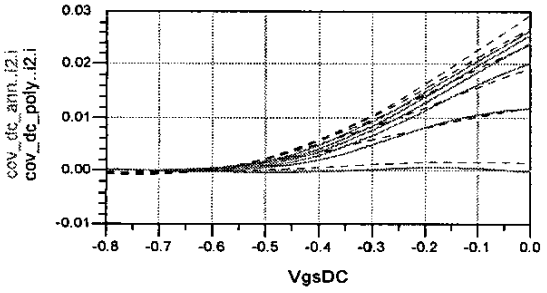

Fig. 3. Comparison of the ANN- (solid line) and poly-nomial-based (dashed line) DC simulation results of I_2 [A]. V_{dsDC} ranges from 0 to 1 V in steps of 0.2 V.

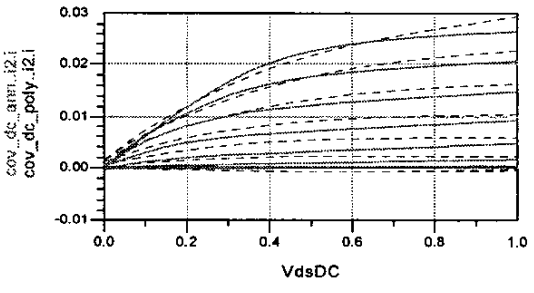

Fig. 4. Comparison of the ANN- (solid line) and poly-nomial-based (dashed line) DC simulation results of I_2 [A]. V_{gsDC} ranges from –0.8 to 0 V in steps of 0.1 V.

IV. Comparison Metrics

We consider two comparison metrics [17] to evaluate the differences between measured (x) and simulated ($\hat{x}$) values in the frequency domain:

1) the natural metric

$$S(x,\hat{x}) = \left|x_0 - \hat{x}_0\right|^2 + 2\sum_{i=1}^{N}\left|x_i - \hat{x}_i\right|^2 \tag{2}$$

2) a weighted metric

$$S(x,\hat{x}) = \left|x_0 - \hat{x}_0\right| + \sum_{i=1}^{N}\frac{\left|x_i\right|}{\sum_{j=1}^{N}\left|x_j\right|}\left|x_i - \hat{x}_i\right| \tag{3}$$

The value S summarises the differences between modelled and measured complex wave-variables components x, where i and j are harmonics indices, N is the number of harmonics considered, and the subscript 0 denotes the DC value. We decided to put the DC contribution outside the summation, because they might mask differences in the higher order harmonics. In the case of the natural metric, all finite-order harmonics are treated equally, so it is directly related to the corresponding differences in time-domain waveforms, whereas in the case of the weighted metric, errors in predicting the dominant harmonics have a relatively larger contribution to the overall metric value. Setting a preference for either of the metrics is not straightforward, as it depends on the model application. When the harmonics with a lower power level are as important as the high-power harmonics (e.g., in mixer applications), then the natural metric may be preferred.

Table 1 lists the calculated comparison metrics according to the values of the scattered travelling voltage waves b_1 and b_2, using the two respective models. A smaller metric value denotes closer agreement between measured and modelled b_i. We note that the observations of the previous section are confirmed, as the ANN outperforms the polynomial-based results. We also see that both models predict b_1 better than b_2.

	B_1		b_2	
	polynomial model	ANN	polynomial model	ANN
natural metric [V^2]	2.7E-5	1.5E-5	1.1E-2	2.0E-3
weighted metric [V]	1.7E-3	5.7E-4	4.0E-2	9.8E-3

Table 1. Comparison metrics for the polynomial- and ANN-based HEMT models. The considered experimental conditions are: V_{gsDC} = -0.4 V, V_{dsDC} = 0.7 V, f_0 =1.8 GHz, a_1 = -3.9 dBm, a_2= -0.7 dBm, $\phi(a_2)-\phi(a_1)$=22°.

V. Conclusions

We have presented a methodology for developing time-domain behavioural models for nonlinear microwave devices, directly from vectorial large-signal measurements. Using DC and large-signal results, we showed that ANN-based model representations outperform multivariate polynomials, due to their sigmoid function-based formulation. This has been further analysed by the introduction and interpretation of metrics to compare the two types of nonlinear models.

Acknowledgements

D. Schreurs is supported by the Fund for Scientific Research-Flanders as a post-doctoral fellow. K.U.Leuven acknowledges Agilent Technologies for the donation of the NNMS, as well as support to implement the models into ADS. The authors also thank Dom Vecchia and Kevin Coakley of NIST for the interesting discussions.

References

[1] F. van Raay and G. Kompa, "A new on-wafer large-signal waveform measurement system with 40 GHz harmonic bandwidth," *IEEE MTT-S Int. Microwave Symp. Dig.*, pp. 1435-1438, 1992.

[2] M. Demmler, P. Tasker, and M. Schlechtweg, "A vector corrected high power on-wafer measurement system with a frequency range for the higher harmonics up to 40 GHz," *Proc. European Microwave Conference*, pp. 1367-1372, 1994.

[3] C. Wei, Y. Lan, J. Hwang, W. Ho, and J. Higgins, "Wave-form characterization of microwave power heterojunction bipolar transistors," *IEEE MTT-S Int. Microwave Symp. Dig.*, pp. 1239-1242, 1995.

[4] J. Verspecht, P. Debie, A. Barel, and L. Martens, "Accurate on wafer measurement of phase and amplitude of the spectral components of incident and scattered voltage waves at the signal ports of a nonlinear microwave device," *IEEE MTT-S Int. Microwave Symp. Dig.*, pp. 1029-1032, 1995.

[5] D. Schreurs, "Overview of large-signal measurements based equivalent circuit and behavioural modelling techniques with regard to non-linear circuit design enhancement," *Proc. IMS2001 Workshop "New Advances in Nonlinear Circuit Design"*, pp. 100-135, 2001.

[6] M. Curras-Francos, P. Tasker, M. Fernandez-Barciela, Y. Campos-Roca, and E. Sanchez, "Direct extraction of nonlinear FET Q-V functions from time domain large-signal measurements," *IEEE Microwave and Guided Wave Letters*, pp. 531-533, 2000.

[7] D. Schreurs and J. Verspecht, "Large-signal modelling and measuring go hand-in-hand: accurate alternatives to indirect S-parameter methods," *International Journal of RF and Microwave Computer-Aided Engineering*, pp. 6-18, 2000.

[8] J. Verspecht, F. Verbeyst, M. Vanden Bossche and P. Van Esch, "System level simulation benefits from frequency domain behavioral models of mixers and amplifiers," *Proc. European Microwave Conference*, pp. 29-32, 1999.

[9] D. Schreurs, J. Wood, N. Tufillaro, D. Usikov, L. Barford, and D.E. Root, "The construction and evaluation of behavioral models for microwave devices based on time-domain large-signal measurements," *Proc. IEEE International Electron Devices Meeting (IEDM)*, pp. 819-822, 2000.

[10] H. Kantz and T. Schreiber, *Nonlinear Time Series Analysis*, Cambridge University Press, 1997.

[11] D. Schreurs, S. Vandenberghe, J. Wood, N. Tufillaro, L. Barford, and D.E. Root, "Automatically controlled coverage of the voltage plane of quasi-unilateral devices," *57th Automatic RF Techniques Group Conference (ARFTG) Dig.*, pp. 86-90, 2001.

[12] M. Kennel, R. Brown, and H. Abarbanel., "Determining embedding dimension for phase-space reconstruction using a geometrical construction," *Phys. Rev. A*, pp. 3403-3411, 1992.

[13] Q.J. Zhang and K.C. Gupta, *Neural networks for RF and microwave design*, Artech House, 2000.

[14] NeuroModeler, ver. 1.2, Q. J. Zhang and his neural network research team, Department of Electronics, Carleton University, Ottawa, Canada, 1999.

[15] V. Devabhaktuni, M. Yagoub, and Q.-J. Zhang, "A robust algorithm for automatic development of neural-network models for microwave applications," *IEEE Trans. Microwave Theory Techn.*, pp. 2282-2291, 2001.

[16] A. Pekker, J. Wood, and D.E. Root, unpublished, private communication, 2001.

[17] K. Remley, J. Jargon, D. Schreurs, D. DeGroot, and K.C. Gupta, "Repeat measurements and metrics for nonlinear model development," *IEEE Int. Microwave Symp. Dig.*, 2-7 June 2002.